Cancer stem cells: Mediators of tumorigenesis and metastasis in head and neck squamous cell carcinoma

Steven B. Chinn, MD,[1] Owen A. Darr, MD,[1] John H. Owen, MS,[1] Emily Bellile, MS,[2] Jonathan B. McHugh, MD,[3] Matthew E. Spector, MD,[1] Silvana M. Papagerakis, MD, PhD,[1] Douglas B. Chepeha, MD,[1] Carol R. Bradford, MD,[1] Thomas E. Carey, PhD,[1] Mark E. P. Prince, MD[1*]

[1]Department of Otolaryngology – Head and Neck Surgery, University of Michigan, Ann Arbor, Michigan, [2]Comprehensive Cancer Center Biostatistics Unit, University of Michigan, Ann Arbor, Michigan, [3]Department of Pathology, University of Michigan, Ann Arbor, Michigan.

Accepted 7 January 2014
Published online 25 March 2014 in Wiley Online Library (wileyonlinelibrary.com). DOI 10.1002/hed.23600

ABSTRACT: *Background.* Cancer stem cells (CSCs) represent a subpopulation of cells responsible for tumor growth. Their role in head and neck squamous cell carcinoma (HNSCC) tumorigenesis and metastasis remains uncertain.

Methods. Wound healing and an orthotopic animal model were used to study cells expressing the CSC phenotype ($CD44^{high}$ and aldehyde dehydrogenase $[ALDH]^{+}$) and assess mobility, tumorigenesis, and metastasis. A prospective collection of 40 patient-derived primary HNSCC specimens were analyzed for CSC-proportion compared to clinical variables.

Results. CSCs exhibited significantly faster wound closure and greater tumorigenesis and regional metastasis in vivo than non-CSCs. In primary patient tumors, size and advanced stage were correlated with elevated proportion of CSCs, however, not with survival.

Conclusion. HNSCC stem cells mediate tumorigenesis and regional metastasis in vivo. In primary patient tumors, CSC-proportion was associated with tumor size and stage, but not with metastatic spread or survival. CSC burden alone may only represent a minor variable in understanding CSCs and metastasis. © 2014 Wiley Periodicals, Inc. *Head Neck* **37:** 317–326, 2015

KEY WORDS: cancer stem cells, CD44, head and neck squamous cell carcinoma, metastasis, animal model

INTRODUCTION

In the stochastic model of tumorigenesis, all cancer cells in a tumor population are capable of initiating tumor growth. The cancer stem cell (CSC) theory of tumorigenesis has recently gained popularity because of identification of a rare subset of cells, CSCs, with the ability for self-renewal, regeneration of a heterogeneous tumor cell population, and the ability to initiate tumors in vivo. The CSC theory holds that this subpopulation of cells are responsible for tumor growth and spread, whereas non-CSCs have limited capacity for regeneration of progeny or the ability to recapitulate a tumor.[1]

Head and neck squamous cell carcinoma (HNSCC) affects over 40,000 Americans with 11,000 dying annually.[2] Regional lymphatic metastasis predisposes patients to the development of distant metastasis, effectively reducing survival rates by 50%.[3–6] Despite advances in treatment, overall survival remains static.[2] Regional and distant metastases make up a considerable proportion of the treatment failures.[6] It is important to study factors associated with cancer spread to develop more effective diagnostic techniques and to identify therapeutic targets. Subpopulations of tumor cells with highly tumorigenic behavior can be identified in HNSCC based on the cellular markers CD44 and aldehyde dehydrogenase (ALDH).[7–11]

CSCs have been identified in solid tumors, including breast, prostate, and pancreatic carcinoma.[11–13] We have previously demonstrated that a subset of HNSCC cells that express CD44 and ALDH have increased self-renewal, tumorigenicity, and the ability to recapitulate a heterogeneous tumor compared with cells without these markers in a flank injection mouse model.[8,9] Cancer cells without these markers had limited or no tumorigenic potential. Additional work using a mouse tail vein injection model of CSC-mediated metastasis demonstrated that HNSCC cells expressing $CD44^{high}$ and $ALDH^{+}$ have a greater capacity to colonize the lungs compared to $CD44^{low}$ and $ALDH^{-}$ tumor cells, which rarely if ever lead to successful lung colonization.[14] In addition, in vitro experiments have shown that HNSCC stem cells have increased motility and invasive characteristics in vitro compared to non-CSCs.[14,15]

***Corresponding author:** M. E. Prince, Department of Otolaryngology – Head and Neck Surgery, University of Michigan, 1500 E. Medical Center Drive, Ann Arbor, MI 48103. E-mail: mepp@med.umich.edu

This work was presented at the 8th International Conference on Head and Neck Cancer, Toronto, Ontario, Canada, July 2012.

Contract grant sponsor: T32 training grant (T32 DC005356); NIDCR 1 R01-DE019126; and University of Michigan Specialized Program of Research Excellence (P50 CA97248).

Additional Supporting Information may be found in the online version of this article.

However, spontaneous metastasis from tumors initiated by head and neck CSCs has not been shown. CSCs may play a key role in metastasis and may serve as a novel target for therapy. CSCs are thought to be slowly replicating cells that have innate chemotherapy and radiation resistance mechanisms. That behavior is a plausible mechanism for treatment failures.[12,16] Development of a physiologic model of metastasis using CSCs is vital to demonstrate the role of CSCs in metastasis and understand the mechanisms of metastasis. More importantly, such a model can be used to develop novel strategies toward cancer therapy. In this article, we will test the hypotheses that (1) CSCs have a greater migratory rate compared to non-CSCs in vitro, (2) CSCs have a greater capacity for tumorigenesis and spontaneous metastasis using an orthotopic tip of the tongue mouse model, and (3) CSC enrichment is associated with metastasis and outcome.

MATERIALS AND METHODS

Patient data and tumor collection

Approval for use of patient data and specimen collection were approved by the University of Michigan's Institutional Review Board and all patients signed written informed consent for the study as part of the University of Michigan Head and Neck Specialized Program of Research Excellence. Forty patients with HNSCC were prospectively collected from 2007 to 2012 (mean age, 57.5 years; M:F ratio, 25:15; median follow-up, 0.8 years). Primary tumors (31 oral cavity, 8 laryngeal, 1 oropharyngeal) were harvested directly from tumor resection specimens. Tumor specimens were taken directly from the operating room and placed in 10% Dulbecco modified Eagle's Medium (DMEM) with 2% calf serum with amphotericin-B. Tumors were then cut into fine pieces with a scalpel and subjected to 2 hours of digestion with collagenase-hyaluronidase enzyme. Specimens were then placed into cell culture flasks with 10% DMEM and left undisturbed for 48 hours in a cell culture incubator. Cells were sorted by flow cytometry for CD44 expression. Tumor CSC enrichment was determined based on the percentage of tumor specimen cells expressing high levels (top 1%) of CD44 based on flow. CD44 expression percentage quartiles were then identified to categorize tumor specimens for analysis. CSC enrichment and clinical covariates (T and N classification, American Joint Committee on Cancer [AJCC] stage, age, tobacco use, perineural invasion [PNI], distant metastasis, tumor size, and tumor depth) were analyzed. Kaplan–Meier survival statistics were used to evaluate overall survival (OS), disease-specific survival (DSS), and disease-free interval.

Cell lines and cell culture

UM-SCC-47 and UM-SCC-103 are well-established HNSCC cell lines derived from advanced stage oral cavity squamous cell carcinomas.[17,18] Both cell lines were transfected with a luciferase cassette (luc+) for bioluminescence imaging, and were grown as previously described to 70% to 80% confluency, trypsinized, and sorted by flow cytometry for injection or plated for wound healing assays.[14]

Flow cytometry

CSCs and non-CSCs were identified and sorted by flow cytometry based on cellular expression patterns of CD44 and ALDH, as reported previously.[7–9,14] ALDH activity was identified in the UM-SCC-47-luc+ and UM-SCC-103-luc+ cancer cell line using the ALDEFLUOR substrate in accord with the manufacturer's protocol (StemCo Biomedical, Durham, NC). Specimens being analyzed for ALDH activity were then counterstained with anti-CD44 (allophycocyanin conjugated; BD Pharmingen, San Diego, CA) at the appropriate dilution. Nonviable cells are eliminated using 4′,6-diamidino-2-phenylindole (DAPI; BD Pharmingen). The specific flow cytometry gates for $ALDH^+$ cells were set using a control sample of isolated tumor cells in which ALDH activity was inhibited with diethylaminobenzaldehyde. Cells expressing CD44 were identified using a fluorescent conjugated anti-CD44 antibody (allophycocyanin conjugated, mouse antihuman, clone G44-26; BD Pharmingen) at a 1:50 dilution for 15 to 20 minutes. Subsequent flow cytometry runs were used to identify populations of cells with positive ALDH activity ($ALDH^+$), negative ALDH activity ($ALDH^-$) (Supplemental Figure 1A and 1B, online only), and cells that express high levels of CD44 ($CD44^{high}$) and low levels of CD44 ($CD44^{low}$) (Supplemental Figure 1C and 1D, online only). For double sorts using both CD44 and ALDH, CD44 expression was identified first followed by subsequent ALDH activity. Cells with $CD44^{high}/ALDH^+$ were analyzed as CSC and $CD44^{low}/ALDH^-$ were analyzed as non-CSCs.

For the wound healing assay, UM-SCC-47-luc+ and UM-SCC-103-luc+ were sorted by flow cytometry, as described above for CD44 activity. Sorted cells (6×10^4 cells/well) were then placed into 24-well culture plates with 10% Dulbecco modified Eagle's medium and allowed to grow to 90% to 100% confluency. A 200 uL pipette tip was then used to make 2 parallel wounds per well. Cells were then observed and the area of the wound was measured at time 0, 9, 15, 18, 20, 24, 26, and 28 hours. The area of the open wound was calculated using the NIH ImageJ free software analysis.[19] Percent closure was calculated based on the area of the wound at the times of interest divided by the area of time 0 for each wound. Time to 100% closure of the wound and mean percent closure at each time point were measured.

Orthotopic mouse model

Approvals for the use of the animal model and for collection of cancer specimens were obtained through the University of Michigan's Committee on Use and Care of Animals and the Institutional Review Board, respectively. Six to 8-week-old NOD/SCID mice were anesthetized with 30–100 mg/kg ketamine and 10 mg/kg xylazine intraperitoneal injections. UM-SCC 47 cells were then injected into the tip of the tongue submucosally. The range of cell numbers injected was 500–1×10^5 sorted and unsorted cells. The animals were observed for primary tumor growth in the tip of the tongue and for regional metastasis using bioluminescence.[10] Evaluation of successful tumor placement was determined by bioluminescence imaging on postinjection day number 1.

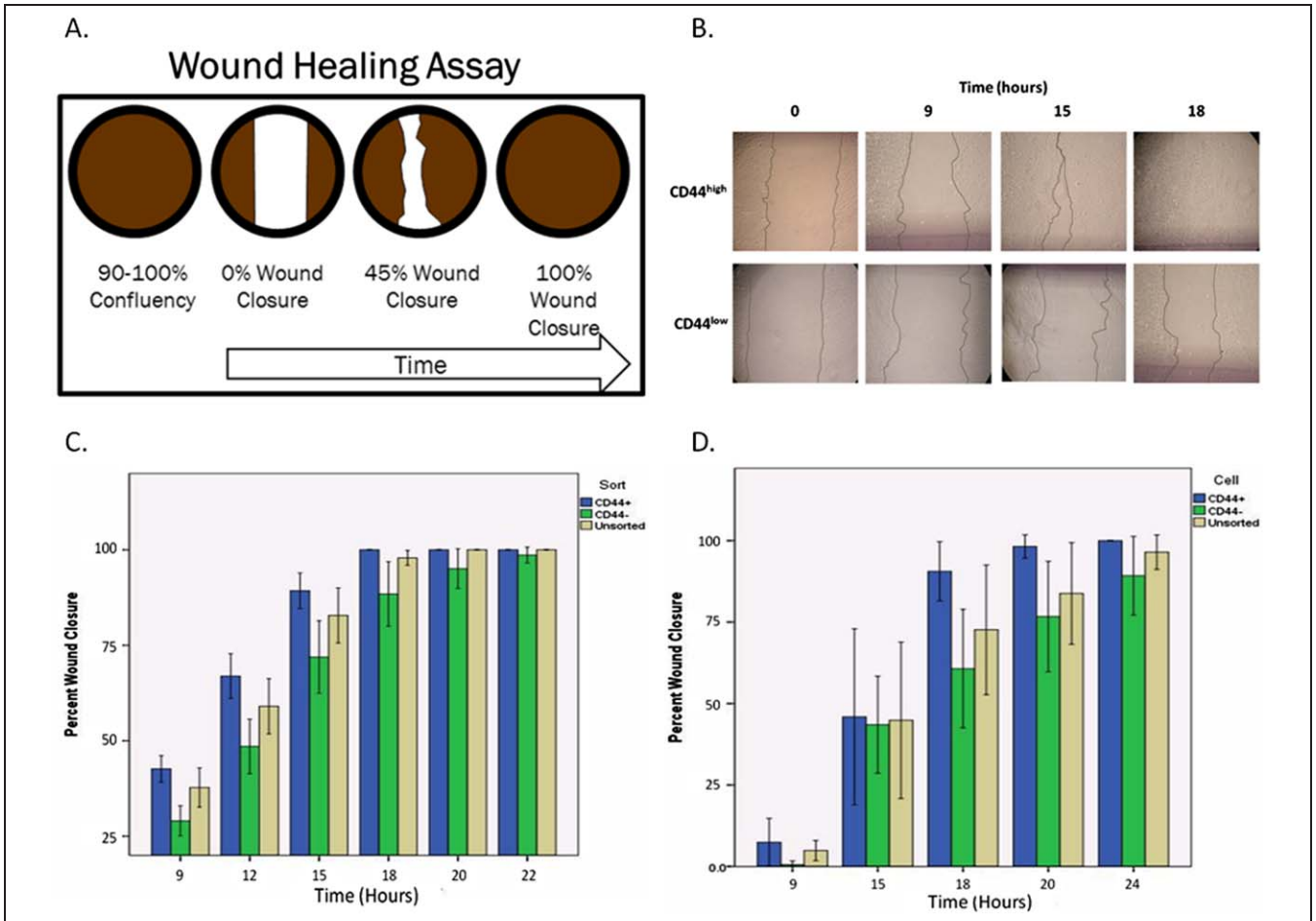

FIGURE 1. Wound healing assay. (A) Experimental design. (B) Representative wound closure over time between CD44high and CD44low cells. Mean percent wound closure for (C) UM-SCC-47 and (D) UM-SCC-103 cells sorted by CD44. Error bars represent standard error. [Color figure can be viewed in the online issue, which is available at wileyonlinelibrary.com.]

Tumor growth at the primary site and metastasis was confirmed by clinical palpation and bioluminescence imaging. Growth of the primary tumors and metastases were monitored weekly for up to 12 weeks by measuring tumor diameters with bioluminescence imaging. A partial glossectomy was performed at 14 to 28 days after injection to reduce tumor burden and improve the animal's ability to tolerate an oral diet and reduce upper airway obstruction.[20] Glossectomy specimens were taken for histologic analysis.

The animals were euthanized and histologic analysis of all tumors was performed to assess gross and histologic evidence of primary tumor growth, to confirm recapitulation of a heterogeneous tumor, confirm bioluminescence imaging regional or pulmonary metastasis, and to evaluate for renewal of CSCs based on flow cytometry. All histology slides were reviewed by a head and neck pathologist (J.B.M.). Outcomes of interest were rate of tumorigenesis (bioluminescence imaging intensity at weekly intervals), time to regional metastasis (time from injection to first identifiable metastasis by bioluminescence imaging), rate of metastatic growth (bioluminescence imaging intensity of regional metastasis at weekly intervals), and development of distant metastasis (time from injection to identification of distant metastasis by bioluminescence imaging).[21]

Luciferase transfection and bioluminescent imaging

The cell lines used in this study were transfected with luciferase to provide in vivo imaging to assess potential metastasis, as previously described.[7–9,14] Mice were anesthetized with isofluorane and placed in the bioluminescent imaging machine to evaluate primary tumor growth and metastasis based on total number of photons/second.[22] To control for background variation, a ratio of tumor region of interest/background control were calculated and recorded to assess for growth.

Primary tumor growth and metastasis in the luciferase-transfected CSC lines injected into the mouse model was monitored with weekly bioluminescence imaging. An area around the tumor and metastasis as demonstrated by bioluminescence imaging was observed and a region of interest was defined around the tumor luminescence. Total and average photons/second were recorded and standardized to background luminescence to quantify and analyze primary growth and regional metastasis for statistical analysis.

Statistical analysis

Wound-healing assays were measured based on mean time to 100% closure and percent-closure at each individual time point. The *t* test was used to calculate differences between means. Outcome measures were bioluminescence imaging intensity (photons/second), intensity over time (days), and time to metastasis. Bioluminescence imaging intensity was measured as average photons/second over time and log-transformed for comparison. A mixed model approach was used to test differences in intensity and differences over time (days) between the CSC versus the non-CSC groups. Kaplan–Meier survival statistics were used to evaluate time to metastasis among CSCs and non-CSCs and an unsorted control group. Patients were grouped based on clinical covariates of interest and CD44 expression was calculated. The *t* test was used to calculate differences between means. Tumor size and CD44 expression were then analyzed as continuous values. Pearson's correlation was then used to calculate correlation coefficient between tumor size and CD44 expression. For survival analysis, CD44 expression was grouped into $CD44^{high}$ and $CD44^{low}$ groups based on percentile rank; $\geq$50th percentile was calculated as $CD44^{high}$ and $<$50th percentile was calculated as $CD44^{low}$. Kaplan–Meier survival statistics were used to calculate OS (time from definitive cancer treatment to death of any cause), DSS (time from definitive treatment to death from disease), and disease-free interval (time from definitive treatment to recurrence of disease). Any p value $< .05$ was considered statistically significant.

RESULTS

In vitro analysis of cancer stem cell motility

To evaluate CSC mobility, wound healing assays were performed using $CD44^{high}$ versus $CD44^{low}$ cells isolated from UM-SCC-47-luc+ and UM-SCC-103-luc+ (Figure 1A). Figure 1B shows representative photographs of the wound healing assay for UM-SCC-47 and UM-SCC-103. Figure 1C summarizes UM-SCC-47 mean percentage of wound closure over time. UM-SCC-47 cells sorted for $CD44^{high}$ expressing cells demonstrated significantly greater mean percentage of wound closure compared to the $CD44^{low}$ expressing cells at 9, 15, 18, and 20 hours ($p = .0001$; .001; .004; and .038, respectively). $CD44^{high}$ UM-SCC-103 cells demonstrated significantly greater mean percentage of wound closure compared to $CD44^{low}$ cells at 9, 18, and 20 hours ($p = .012$; .012; and .036, respectively; Figure 1D). The mean time to closure was significantly shorter in cells sorted for $CD44^{high}$ compared to $CD44^{low}$ sorted cells for both UM-SCC-47 (17.8 hours vs 21 hours; $p = .001$) and UM-SCC-103 cell lines (20.6 hours vs 25.8 hours; $p = .028$).

Orthotopic mouse model: Tumorigenesis

An orthotopic mouse model was generated based on previous work by Sano and Myers.[18] UM-SCC-47-luc+, 1×10^5 unsorted cells were injected into the tip of the tongue in NOD/SCID mice (Figure 2A). Tumor growth was measured by luminescence (photons/second) at the primary site and regional lymph nodes (Figure 2B). To estimate the relative bioluminescence per cell, a known number of UM-SCC-47-luc+ cells were examined for bioluminescence intensity in vitro. Primary tumor and lymph nodes were examined on hematoxylin-eosin–stained sections to confirm the presence of squamous cell carcinoma (Figure 2C).

The relative capacity of CSCs and non-CSCs to generate tumors was compared using the orthotopic mouse model. Tumor cells were sorted to obtain $CD44^{high}$, $CD44^{low}$, $CD44^{high}/ALDH^+$, $CD44^{low}/ALDH^-$, and unsorted control populations. To compare tumorigenic potential of $CD44^{high}$ and $CD44^{low}$ cells, population sizes ranging from 500–25,000 UM-SCC-47-luc+ cells/injection were analyzed. The minimum number of cells to produce a tumor was 50-fold lower for $CD44^{high}$ UM-SCC-47-luc+ cells compared to the $CD44^{low}$ cells (500 vs 25,000). Furthermore, primary tumor growth at 28 days was demonstrated in all of 5 mice injected with $CD44^{high}$ cells versus only 1 of 4 mice injected with $CD44^{low}$ cells ($p = .047$). Similarly, there was a greater capacity for tumor growth in mice injected with 2.5×10^4 $CD44^{high}/ALDH^+$ cells compared to $CD44^{low}/ALDH^-$ at 28 days postinjection (2 of 2 vs 0 of 2, respectively; Table 1). The rate of tumor take and growth after injecting 2.5×10^4 CD44 sorted cells was significantly higher in the $CD44^{high}$ and $CD44^{high}/ALDH^+$ populations compared to $CD44^{low}$ and $CD44^{low}/ALDH^-$ populations ($p = .0011$). Comparison of bioluminescence at individual time points demonstrated significantly higher levels of luminescence (photons/second) in the primary tumors generated by $CD44^{high}$ and $CD44^{high}/ALDH^+$ cells at days 21, 28, 36, and 43 compared to $CD44^{low}$ and $CD44^{low}/ALDH^-$ cells. Collectively, CSCs ($CD44^{high}$ and $CD44^{high}/ALDH^+$) had significantly greater capacity for tumorigenesis and greater rates of tumor growth compared to non-CSCs ($CD44^{low}$ and $CD44^{low}/ALDH^-$; Figure 3A and 3C).

Histologic evaluation of the $CD44^{high}$ and $CD44^{high}/ALDH^+$ derived primary tumors demonstrated invasive moderately differentiated squamous cell carcinoma with perineural invasion (Figure 3B). These results strongly suggest cells expressing high levels of the CSC marker CD44 and ALDH have greater tumorigenic potential compared to cells expressing $CD44^{low}$ or $CD44^{low}/ALDH^-$. High tumorigenic potential in $CD44^{high}$and $CD44^{high}/ALDH^+$ cells further supports CD44 and ALDH as markers for head and neck CSCs.

Orthotopic mouse model: Metastasis

Mice injected with 2.5×10^4 $CD44^{high}$ or $CD44^{high}/ALDH^+$ cells were assessed for metastatic potential relative to $CD44^{low}$ or $CD44^{low}/ALDH^-$ cells. All mice injected with $CD44^{high}$ or $CD44^{high}/ALDH^+$ had a significantly shorter metastasis-free interval compared with mice injected with $CD44^{low}$ or $CD44^{low}/ALDH^-$ cells (mean time to metastasis 21.6 vs 40 days; $p = .005$; Figure 4A). There was significantly greater regional metastatic luminescence in $CD44^{high}$ and $CD44^{high}/ALDH^+$ cells injections at 28, 36, and 43 days compared to $CD44^{low}$ and $CD44^{low}/ALDH^-$ (Figure 4B and 4C). Histologic analysis of the lymph nodes confirmed the bioluminescence imaging results and the development of spontaneous metastasis of squamous cell carcinoma (Figure 4D).

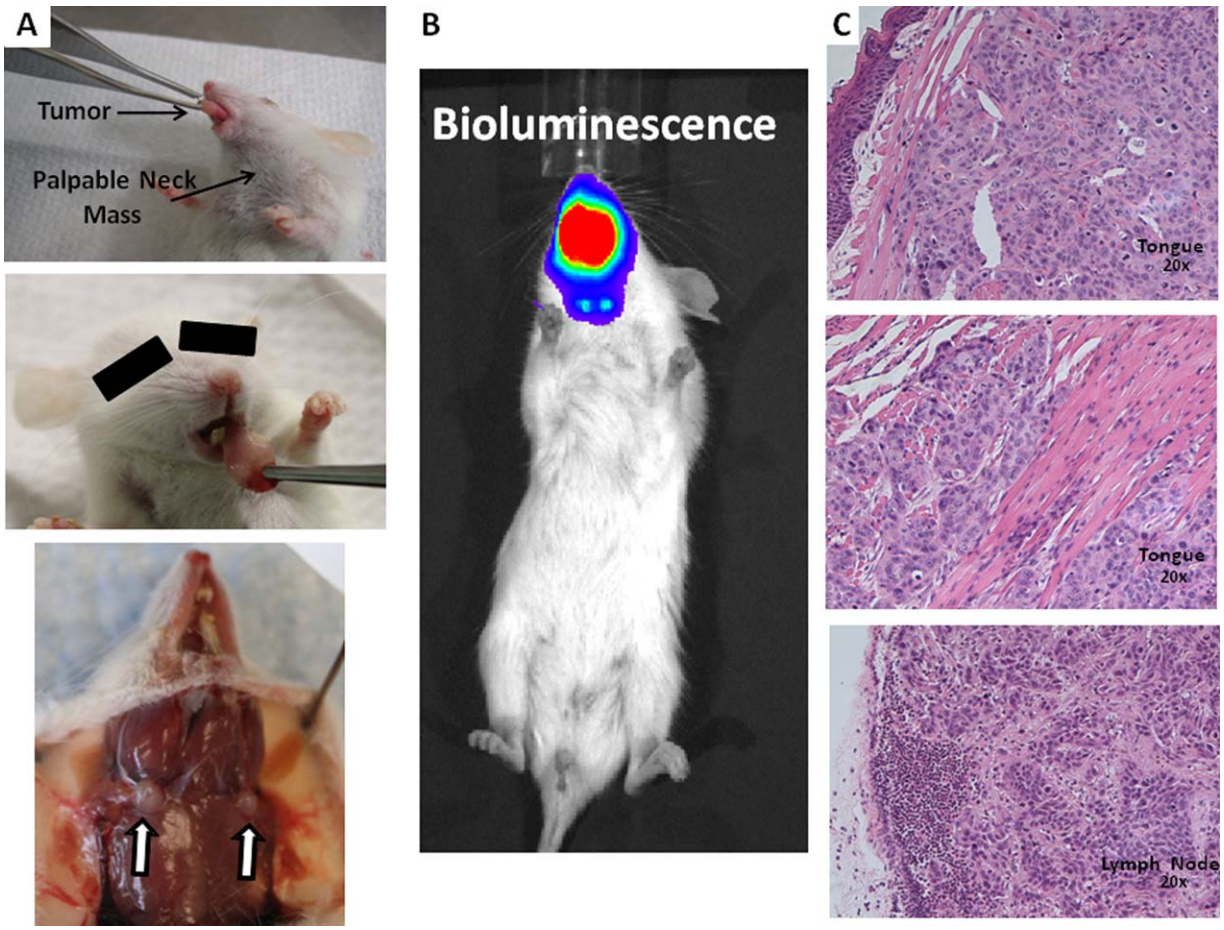

FIGURE 2. Validation of orthotopic mouse model. (A) Gross examination of primary tongue tumor growth with palpable neck mass. Postmortem neck dissection with visible enlarged lymph nodes (white arrows). (B) Bioluminescent imaging with high intensity (red) primary tumor and 2 areas of increased intensity around cervical lymph nodes. (C) Hematoxylin-eosin staining demonstrates invasive moderately differentiated squamous cell carcinoma (SCC) with perineural invasion of the primary tumor and metastatic SCC to lymph nodes. [Color figure can be viewed in the online issue, which is available at wileyonlinelibrary.com.]

A distant metastasis was detected by luminescence in a $CD44^{high}/ALDH^{+}$ mouse that could be kept alive for 71 days postinjection and 38 days postglossectomy. Bulky lymphadenopathy was seen by luminescence and confirmed by necropsy. Histologic analysis of the regional and distant lung metastasis confirmed spontaneous metastasis of squamous cell carcinoma (Figure 5E). A comparative $CD44^{low}/ALDH^{-}$ mouse that developed a primary tumor significantly delayed after injection was kept alive for a similar length of time and did not develop distant metastasis.

TABLE 1. Tumorigenesis: Number of primary tongue tumors resulting from implantations of cancer stem cells ($CD44^{high}$ and $CD44^{high}$/aldehyde dehydrogenase^{+}) and non-cancer stem cells ($CD44^{low}$ and $CD44^{low}$/aldehyde dehydrogenase^{-}).

Number of cells/injection	CSC	Non-CSC	Control
1×10^5	--	--	2/2
5×10^4	2/2	2/2	1/1
2.5×10^4	5/5	1/4	1/1
1×10^3	1/1	0/1	--
500	1/1	0/1	--

Abbreviation: CSC, cancer stem cell.
Note: Number of tumors derived from tongue injections of CSC ($CD44^{high}$ and $CD44^{high}$/aldehyde dehydrogenase $[ALDH]^{+}$) and non-CSC ($CD44^{low}$ and $CD44^{low}/ALDH^{-}$) cells for each titration of UM-SCC-47 cells.

Patient outcomes and tumor $CD44^{high}$ content

Mean $CD44^{high}$ content of all 40 tumor specimens was 10.8% (range, 0% to 84.5%). There was no statistical difference in mean $CD44^{high}$ content between subsites (oral cavity 12.6%, oropharynx 12.9%, and larynx 3.2%; $p = .436$; Figure 5A). Mean CD44 content in primary tumors relative to regional metastasis, distant metastasis, stage, tumor size, and PNI was evaluated (Figure 5B–5F). Only stage and tumor size were significantly correlated with CD44 content. Advanced stage tumors (AJCC stage III/IV) had significantly elevated CD44 content compared to early stage (AJCC stage I/II; 11.6% vs 1.2%; $p = .002$). Increased tumor size was associated with elevated CD44 content ($p = .007$). Tumor specimens from patients with regional metastases had higher $CD44^{high}$ content compared to patient specimens without regional metastases;

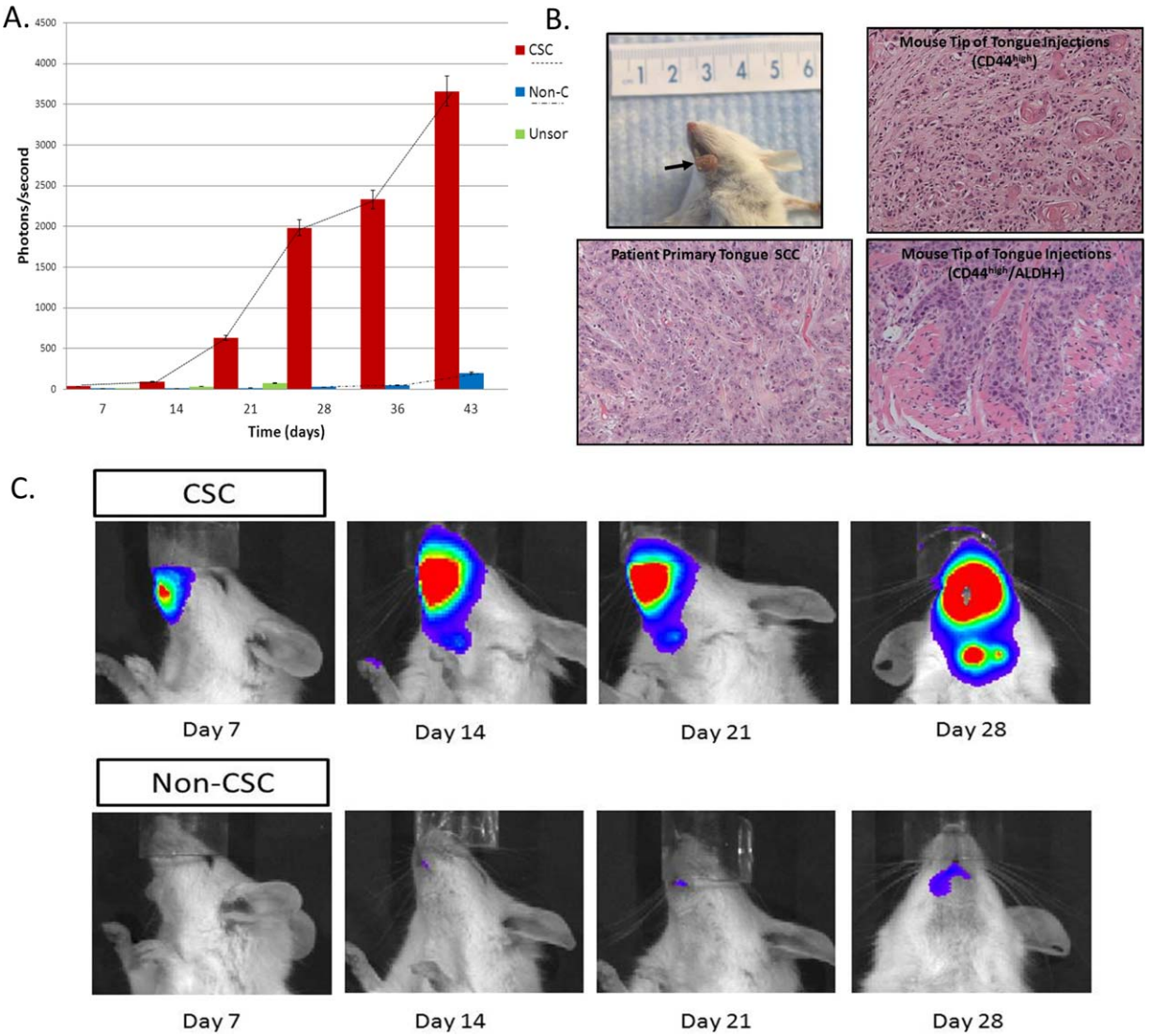

FIGURE 3. Tumorigenesis. (A) Comparison of bioluminescence over time between cancer stem cells (CSC) (red = $CD44^{high}$ and $CD44^{high}$/aldehyde dehydrogenase $[ALDH]^{+}$), non-CSC (blue = $CD44^{low}$ and $CD44^{low}/ALDH^{-}$), and unsorted control (green). (B) Gross (arrow) and histologic comparison of CSC-derived squamous cell carcinoma (SCC) compared to primary patient tumor. (C) Representative bioluminescence imaging of CSC and non-CSC mice at various time points. Error bars represent standard error. [Color figure can be viewed in the online issue, which is available at wileyonlinelibrary.com.]

however, this was not statistically significant (12% vs 9.7%; $p = .70$). Tumor specimens from patients who had at least 2 years of follow-up were analyzed for association of CD44 enrichment and distant metastases. Patients who developed distant metastases had higher CD44 content compared to patient specimens without distant metastases; however, this was not statistically significant (10.2% vs 4.3%; $p = .34$). PNI is a known risk factor for regional metastasis. In patients with PNI, there were higher levels of $CD44^{high}$ content compared to PNI-negative specimens; however, there was no statistical correlation (10.2% and 4.3%; $p = .32$).

Analysis of patient survival outcomes relative to CD44 content was performed (Figure 5G and 5H). There was no difference in OS, DSS, or disease-free interval ($p = .961$; $p = .960$; and $p = .355$, respectively) among patients with elevated CD44 enrichment compared to those with lower CD44 content.

DISCUSSION

CSCs ($CD44^{high}$ and $CD44^{high}/ALDH^{+}$) have significantly increased in vitro migration and wound healing in an orthotopic mouse model are more tumorigenic with a greater rate of spontaneous metastasis compared to non-CSCs ($CD44^{low}$ and $CD44^{low}/ALDH^{-}$). We demonstrate a useful orthotopic mouse model that can be used to study in vivo tumor growth and spontaneous metastasis using a minimal number of CSCs. Additionally, the mouse model has shown the reproducible and reliable ability of CSCs to form regional metastasis. These findings suggest that CSCs ($CD44^{high}$ and $CD44^{high}/ALDH^{+}$) have a greater

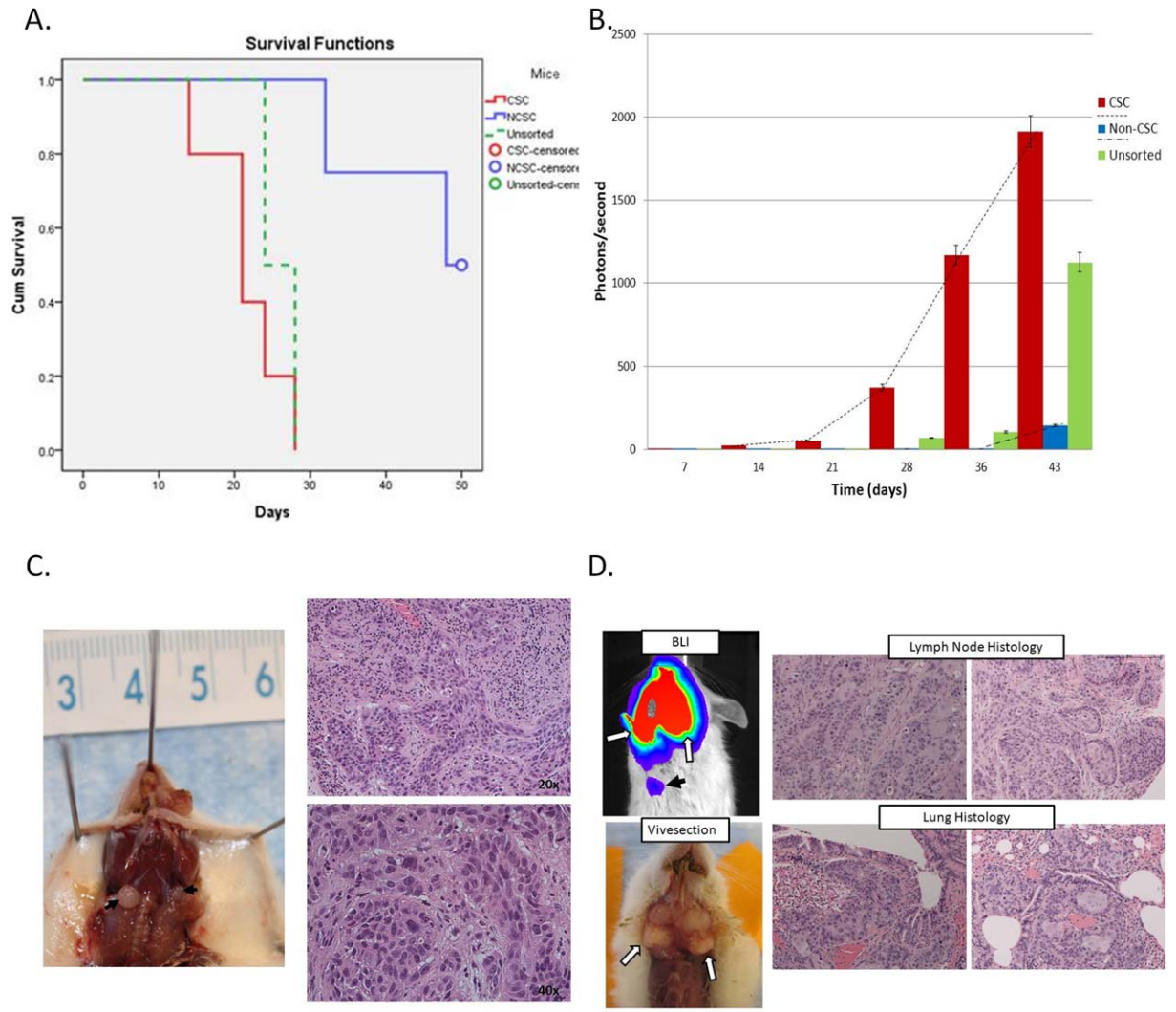

FIGURE 4. Metastasis. (A) Kaplan-Meier analysis of time to regional metastasis between cancer stem cells (CSC) (red = $CD44^{high}$ and $CD44^{high}$/aldehyde dehydrogenase $[ALDH]^{+}$), non-CSC (blue = $CD44^{low}$ and $CD44^{low}/ALDH^{-}$), and unsorted control (green). (B) Comparison of regional metastatic bioluminescence imaging over time between CSC (red = $CD44^{high}$ and $CD44^{high}/ALDH^{+}$), non-CSC (blue = $CD44^{low}$ and $CD44^{low}/ALDH^{-}$), and unsorted control (green). (C) Representative bioluminescence imaging of regional metastasis of CSC at various time points. (D) Gross (black arrowhead) and histologic comparison of $CD44^{high}$-derived spontaneous squamous cell carcinoma (SCC) metastasis. (E) Gross (white arrow) and histologic comparison of $CD44^{high}/ALDH^{+}$-derived spontaneous SCC regional (white arrows) and distant metastasis (black arrows). [Color figure can be viewed in the online issue, which is available at wileyonlinelibrary.com.]

capacity for spontaneous regional and distant metastatic spread and growth compared to non-CSCs ($CD44^{low}$ and $CD44^{low}/ALDH^{-}$). This is an important step in defining the role of CSCs in metastasis and developing a model for future targeted stem cell therapy. In primary patient tumors, CSC enrichment in primary tumors is significantly associated with increased tumor size and tumor stage, whereas there were trends for association of $CD44^{high}$ content with regional and distant metastasis and PNI. $CD44^{high}$ content was not associated with long-term survival.

Work by others in breast, colorectal, and prostate cancers support our findings indicating that CSCs may play a critical role in tumorigenesis, treatment resistance, and metastasis.[11–13,23] We initially sought to evaluate in vitro assays of cell migration via wound healing assay as a proxy to establish CSCs as a more aggressive subtype from a wound healing standpoint. CSCs seem to have a greater rate of wound closure compared to non-CSCs for both UM-SCC-47 and UM-SCC-103. To further validate the in vitro data, a more physiologic model was developed. In head and neck cancer, previous work by Prince et al [8] and Davis et al[14] showed that UM-SCC-47-luc+ ($CD44^{high}/ALDH^{+}$) cells have a significantly greater ability to colonize the lungs after tail-vein injections than $CD44^{high}ALDH^{-}$cells. A common concern for the tail vein injection model is that the lung lesions represent tumor seeding or capillary entrapment rather than overt cancer metastasis and invasion. The tip of the tongue of the orthotopic mouse model addresses the ability for CSC recapitulation of heterogeneous tumors with significantly elevated tumorigenicity at the primary site and a significant ability to form spontaneous regional and distant metastasis.

We have shown that cells expressing high levels of CD44 alone or jointly with elevated ALDH activity have

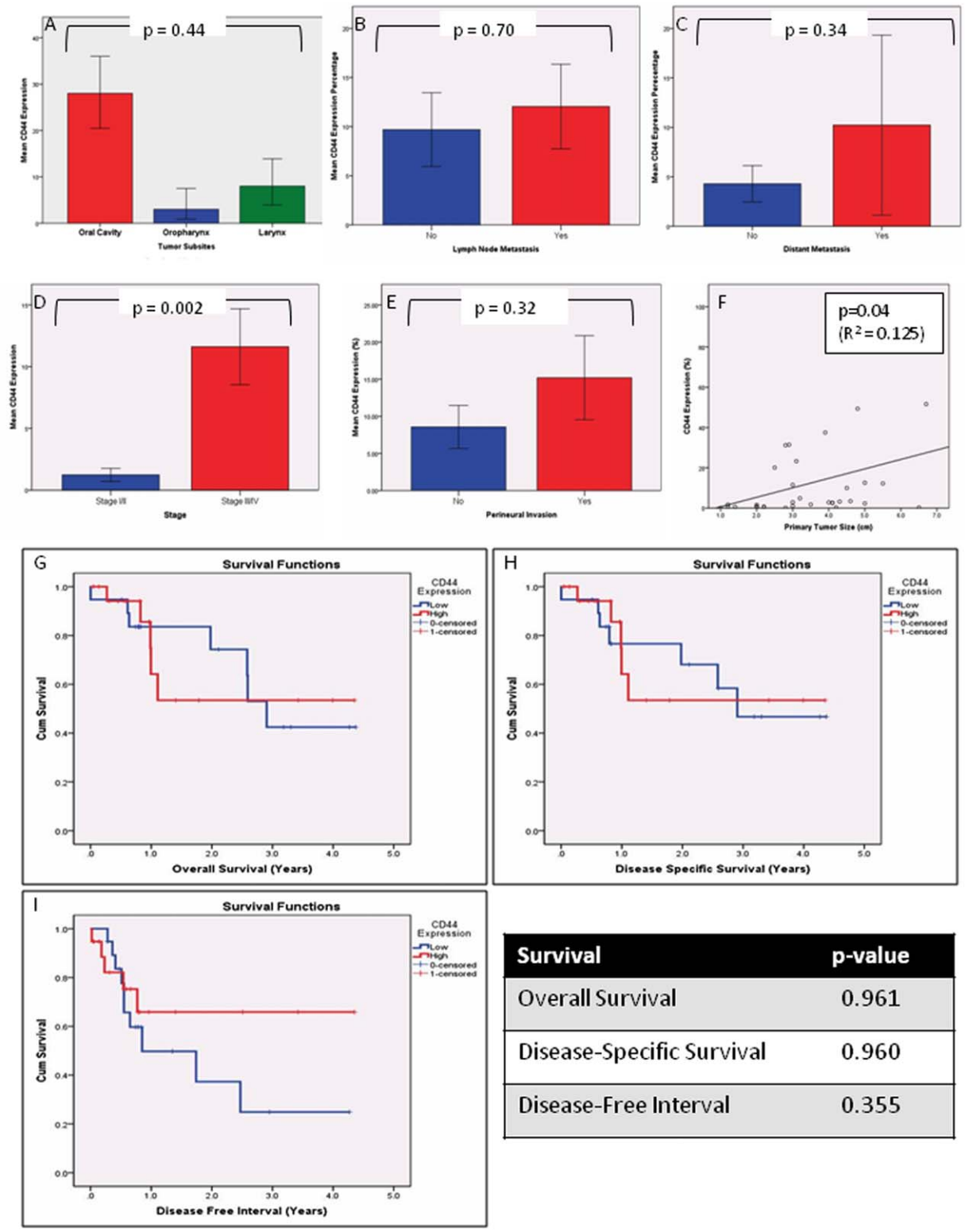

Survival	p-value
Overall Survival	0.961
Disease-Specific Survival	0.960
Disease-Free Interval	0.355

FIGURE 5. Association of clinical variables and CD44 enrichment in patient-derived primary tumor specimens and survival outcome analysis. CD44 enrichment relative to (A) tumor subsite (oral cavity, oropharynx, and glottis); (B) lymph node metastasis; (C) distant metastasis; (D) American Joint Committee on Cancer stage (I/II vs III/IV); (E) perineural invasion; and (F) primary tumor size. Outcome measures of tumor specimens with elevated CD44 enrichment (high) versus low CD44 enrichment (low). (G) Overall survival; (H) disease-specific survival; and (I) disease-free interval. [Color figure can be viewed in the online issue, which is available at wileyonlinelibrary.com.]

a greater ability to form primary tumors and regional metastasis compared to cells lacking these 2 markers. The development of regional metastasis in the CSC group further strengthens the argument that CSCs are an essential regulator and component of metastatic spread. The exact role of CD44 and ALDH in CSC pathophysiology remains unclear. CD44 is a cell surface receptor for the extracellular matrix molecule hyaluronan, with multiple established mechanisms for cancer growth and spread. Specifically, CD44 has been implicated as a cell surface receptor for cell-cell adhesion, cell-matrix adhesion, endothelial attachment and invasion, cell signal transmission, and potent mediator for cell proliferation.[24] Wang et al[24] were able to show that elevated CD44 was associated with worse survival. Over the last several years, its role as a CSC marker has been extensively studied. However, $CD44^{high}$ may not identify all cells with CSC characteristics and has been shown to be a less selective marker of HNSCC than ALDH expression.[8] If sufficient numbers of $CD44^{low}$ cells, such as the experiments in which 2.5×10^4 $CD44^{low}$ non-CSCs could eventually yield tumor growth and regional metastasis over longer periods of time compared to the $CD44^{high}$ CSC group, the addition of ALDH as a second marker for CSC identification can help demonstrate a more specific marker for CSC ability to form primary tumors and regional metastasis.

ALDH is a well-established marker for normal hematopoietic and nervous system stem cells.[25] In addition, ALDH activity has been a significant marker for breast CSCs.[11] Work by Clay et al[9] has shown that ALDH activity is associated with head and neck CSCs and may be a more specific marker for highly tumorigenic cancer cells.[8,9] Although the in vitro wound-healing assay did not assess $CD44^{high}/ALDH^{+}$ versus $CD44^{low}/ALDH^{-}$, we have shown that when using CD44 and ALDH as concurrent CSC markers, there is a greater ability for primary tumor growth and regional metastasis compared to $CD44^{low}/ALDH^{-}$ injections. Failure to generate regional metastasis in the $CD44^{low}/ALDH^{-}$ group as compared to the $CD44^{low}$ only group suggest that ALDH may be a more specific and necessary marker for identifying CSCs and facilitating metastasis. We did not see any gross differences when evaluating $CD44^{high}$ and $CD44^{high}/ALDH^{+}$, however, the overall group was small and subgroup analysis would require a larger sample size. However, the exact role that ALDH plays in CSC tumorigenicity and metastasis remains unclear. Future work evaluating $CD44^{high}/ALDH^{+}$ versus $CD44^{low}/ALDH^{-}$ in vitro may provide a rapid model to further investigate ALDH and CD44 concomitant expression outcomes and potential targets for therapy. Additionally, evaluating for differences between $CD44^{high}$ and $CD44^{high}/ALDH^{+}$ in the animal model may provide additional insight into the true effect of ALDH on metastasis.

One of the weaknesses of this study was the potential for non-CSCs to form tumors and regional metastasis. The capacity for lymph node metastases for non-CSCs were identified and found to be significantly lower compared to CSCs. Despite attempts to isolate 100% CSCs and 100% non-CSCs, the current flow technology does not allow for complete cell expression or marker purity. One can hypothesize that the lymph node growth may represent the impurity of the non-CSC injections. Alternatively, non-CSCs may have a low metastatic potential. This question is interesting and requires future study, particularly given the heterogeneous nature of HNSCC.

Grossly, HNSCC is seen as a heterogeneous tumor with varied clinical outcomes. At the cellular level, it is possible that although CSCs may have the potential for metastatic spread, the CSC population in an individual tumor is highly heterogeneous and not all CSCs are capable of regional or distant metastasis.[26] Although size and stage were associated with enrichment of $CD44^{high}$ cells, there was no statistical association with metastasis and survival. This suggests that increased enrichment of CD44 cells is associated with tumorigenesis, but not with metastasis and outcome. Limitations of the patient data are the number of patients studied. A larger study may identify associations between CD44 enrichment and metastasis and outcome. CD44 has several variants that are associated with survival outcomes.[24] Although the antibodies used for flow did not assess CD44-variants, it is very possible

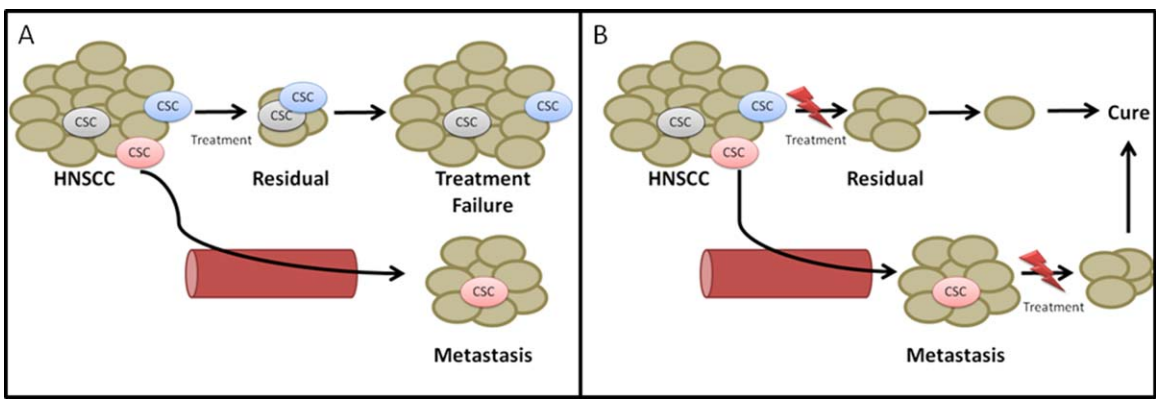

FIGURE 6. Mechanisms of treatment failure and recurrence. (A) A single cancer stem cell (CSC) may be capable of leaving the primary tumor and spreading to regional and distant sites. Current treatment does not fully target CSCs, thus, residual, metastatic, or resistant CSCs are responsible for treatment failure. (B) CSC-specific treatment may lead to improved treatment. HNSCC, head and neck squamous cell carcinoma. [Color figure can be viewed in the online issue, which is available at wileyonlinelibrary.com.]

that CSC CD44-variant expression mediates metastatic potential. All animals injected with UM-SCC-47 had regional disease, whereas the patient population was not as clear based on CD44 expression. CD44 variants, as described by Wang et al,[24] may represent a vital variable with regard to metastatic capability. Future examination of CD44-variant expression within CSCs may further delineate metastatic expression signatures in CSCs. However, taken in context with the in vivo animal study findings that CSCs are necessary for metastasis; one could interpret the patient data to support the theory that a limited number of or even a single CSC is capable of forming metastases and that treatment failure or recurrence may be mediated by a small number of residual CSCs (Figure 6A). Metastatic capacity may not be programmed into every CSC and it may be the continued accumulation of mutations or expression alterations that may activate the ability for particular CSCs to gain invasive capacity and to form metastasis. Identification of the CSC-metastatic genetic signature may yield the best chance for understanding the CSC-specific mechanisms of metastasis and for targeted treatment. Designing CSC-specific signatures and targets may provide novel insight into diagnostics and potentially novel treatment modalities (Figure 6B).

Overall, this study demonstrated the essential role CSCs have in tumorigenesis and, more importantly, as a vital component of the development of metastasis. The development of an animal model with the ability to recreate metastatic disease is an important step for understanding the biology of CSCs and metastatic disease, but more importantly allows for a model to test potential therapeutics targeting head and neck CSCs. Further studies to better define the role that CSCs have in tumorigenesis and metastasis will be critical to developing novel targets for therapy.

REFERENCES

1. Reya T, Morrison SJ, Clarke MF, Weissman IL. Stem cells, cancer, and cancer stem cells. *Nature* 2001;414:105–111.
2. Jemal A, Siegel R, Xu J, Ward E. Cancer statistics, 2010. *CA Cancer J Clin* 2010;60:277–300.
3. Genden EM, Ferlito A, Bradley PJ, Rinaldo A, Scully C. Neck disease and distant metastases. *Oral Oncol* 2003;39:207–212.
4. Kuperman DI, Auethavekiat V, Adkins DR, et al. Squamous cell cancer of the head and neck with distant metastasis at presentation. *Head Neck* 2011; 33:714–718.
5. Layland MK, Sessions DG, Lenox J. The influence of lymph node metastasis in the treatment of squamous cell carcinoma of the oral cavity, oropharynx, larynx, and hypopharynx: N0 versus N+. *Laryngoscope* 2005;115: 629–639.
6. Sano D, Myers JN. Metastasis of squamous cell carcinoma of the oral tongue. *Cancer Metastasis Rev* 2007;26:645–662.
7. Prince ME, Ailles LE. Cancer stem cells in head and neck squamous cell cancer. *J Clin Oncol* 2008;26:2871–2875.
8. Prince ME, Sivanandan R, Kaczorowski A, et al. Identification of a subpopulation of cells with cancer stem cell properties in head and neck squamous cell carcinoma. *Proc Natl Acad Sci U S A* 2007;104:973–978.
9. Clay MR, Tabor M, Owen JH, et al. Single-marker identification of head and neck squamous cell carcinoma cancer stem cells with aldehyde dehydrogenase. *Head Neck* 2010;32:1195–1201.
10. Charafe–Jauffret E, Ginestier C, Iovino F, et al. Aldehyde dehydrogenase 1-positive cancer stem cells mediate metastasis and poor clinical outcome in inflammatory breast cancer. *Clin Cancer Res* 2010;16:45–55.
11. Wicha MS. Cancer stem cells and metastasis: lethal seeds. *Clin Cancer Res* 2006;12:5606–5607.
12. Bao S, Wu Q, McLendon RE, et al. Glioma stem cells promote radioresistance by preferential activation of the DNA damage response. *Nature* 2006; 444:756–760.
13. Vermeulen L, Todaro M, de Sousa Mello F, et al. Single-cell cloning of colon cancer stem cells reveals a multi-lineage differentiation capacity. *Proc Natl Acad Sci U S A* 2008;105:13427–13432.
14. Davis SJ, Divi V, Owen JH, et al. Metastatic potential of cancer stem cells in head and neck squamous cell carcinoma. *Arch Otolaryngol Head Neck Surg* 2010;136:1260–1266.
15. Yu CC, Lo WL, Chen YW, et al. Bmi-1 regulates snail expression and promotes metastasis ability in head and neck squamous cancer-derived ALDH1 positive cells. *J Oncol* 2011;2011.
16. Al-Assar O, Muschel RJ, Mantoni TS, McKenna WG, Brunner TB. Radiation response of cancer stem-like cells from established human cell lines after sorting for surface markers. *Int J Radiat Oncol Biol Phys* 2009;75: 1216–1225.
17. Brenner JC, Graham MP, Kumar B, et al. Genotyping of 73 UM-SCC head and neck squamous cell carcinoma cell lines. *Head Neck* 2010;32:417–426.
18. Lin CJ, Grandis JR, Carey TE, et al. Head and neck squamous cell carcinoma cell lines: established models and rationale for selection. *Head Neck* 2007;29:163–188.
19. Schneider CA, Rasband WS, Eliceiri KW. NIH Image to ImageJ: 25 years of image analysis. *Nat Methods*. 2012;9:671–675.
20. Myers JN, Holsinger FC, Jasser SA, Bekele BN, Fidler IJ. An orthotopic nude mouse model of oral tongue squamous cell carcinoma. *Clin Cancer Res* 2002;8:293–298.
21. Sano D, Myers JN. Xenograft models of head and neck cancers. *Head Neck Oncol* 2009;1:32.
22. O'Neill K, Lyons SK, Gallagher WM, Curran KM, Byrne AT. Bioluminescent imaging: a critical tool in pre-clinical oncology research. *J Pathol* 2010;220:317–327.
23. Liu H, Patel MR, Prescher JA, et al. Cancer stem cells from human breast tumors are involved in spontaneous metastases in orthotopic mouse models. *Proc Natl Acad Sci U S A* 2010;107:18115–18120.
24. Wang SJ, Wong G, de Heer AM, Xia W, Bourguignon LY. CD44 variant isoforms in head and neck squamous cell carcinoma progression. *Laryngoscope* 2009;119:1518–1530.
25. Corti S, Locatelli F, Papadimitriou D, et al. Identification of a primitive brain-derived neural stem cell population based on aldehyde dehydrogenase activity. *Stem Cells* 2006;24:975–985.
26. Schneider BL, Kulesz–Martin M. Destructive cycles: the role of genomic instability and adaptation in carcinogenesis. *Carcinogenesis* 2004;25:2033–2044.